Drying kinetics and shrinkage rate of thin-sliced pears in different drying stages

Article *in* Journal of Food Process Engineering · December 2022

DOI: 10.1111/jfpe.14264

8 authors, including:


Davood Kalantari
Sari Agricultural Sciences and Natural Resources University


Sara Naji-Tabasi
Institute of Food Science and Technology


Mohammad Kaveh
Knowledge University, Erbil, Iraq


Mohsen Azadbakht
Gorgan University of Agricultural Sciences and Natural Resources

Received: 13 June 2022 | Revised: 15 November 2022 | Accepted: 17 December 2022
DOI: 10.1111/jfpe.14264

ORIGINAL ARTICLE

Journal of Food Process Engineering WILEY

Drying kinetics and shrinkage rate of thin-sliced pears in different drying stages

Davood Kalantari[1] | Sara Naji-Tabasi[2] | Mohammad Kaveh[3] | Mohsen Azadbakht[4] | Moein Majnooni[1] | Yuness Khorshidi[1] | Ali Asghari[4] | Esmail Khalife[5]

[1]Department of Biosystems Engineering, Sari Agricultural Sciences and Natural Resources University (SANRU), Sari, Iran

[2]Department of Food Nanotechnology, Research Institute of Food Science and Technology, Mashhad, Iran

[3]Department of Petroleum Engineering, College of Engineering, Knowledge University, Erbil, Iraq

[4]Department of Biosystems Engineering, Gorgan University of Agricultural Sciences and Natural Resources, Gorgan, Iran

[5]Department of Civil Engineering, Cihan University-Erbil, Erbil, Iraq

Correspondence

Davood Kalantari, Department of Biosystems Engineering, Sari Agricultural Sciences and Natural Resources University (SANRU), Sari, Iran.
Email: d.kalantari@sanru.ac.ir

Mohammad Kaveh, Department of Petroleum Engineering, College of Engineering, Knowledge University, Erbil 44001, Iraq.
Email: sirwan.kaweh@knu.edu.iq and sirwankaweh@gmail.com

Abstract

In this research, the effect of different parameters of a convective hot air dryer on the mass transfer coefficients of thin-sliced pears in different drying stages is analytically and experimentally investigated. According to the results, in the first stage of drying which begins from the initial moisture content (MC) of 87–57% in this study, the convective heat transfer coefficient, the inlet air temperature and the initial MC of the product had the highest influence on the mass transfer rate of the drying product. In the second drying stage (from 57 to 27% MC), the structure of internal pore of the fruit, the internal MC and the thickness of the cut layers are the most influencing parameters controlling the mass transfer coefficient of the product. In the third region of drying (from MC of 27% to the final MC), the inlet air temperature had the greatest effect on the rate of mass transfer from the product. In this region of drying, increasing the drying temperature from 50 to 60°C at an airflow velocity of 0.5 m/s, yielded increasing the effective diffusion coefficient from 1.19×10^{-7} to 4.09×10^{-7} m/s^2. The results of this study showed that increasing the airflow rate in the third stage of drying reduces the effective mass transfer coefficient. The highest effective diffusion coefficient in the third region of drying for thin-sliced pears was obtained equal to 6.24×10^{-7} m/s^2 for drying temperature of 80°C and airflow velocity of 0.5 m/s.

Practical Applications

Pears (*Pyrus communis* L.) are bell-shaped fruits that are in the range of green, yellow, brown, red, or a combination of these colors. This useful fruit is rich in potassium, vitamins, and minerals. There are 30 varieties of pears in the world and they are consumed cooked, compote, or raw. The drying process of fruits and vegetables by reducing the moisture of the product, prevents chemical and biochemical spoilage of the product and increases their shelf life. However, some undesirable physical and chemical changes such as discoloration, texture, and nutritional value may also occur during drying, which reduces consumer acceptance. Drying operations usually take place in the final stages and after other operations and lead to the production of the final product.

KEYWORDS
critical moisture, drying kinetics, mass transfer, mathematical model, shrinkage

1 | INTRODUCTION

Increasing population growth and the need for more foodstuffs, and consequently the limitations of energy resources as well as increasing energy costs in the recent years, emphasis the importance of reducing the losses of agricultural products (Qu et al., 2021). One of the most important reasons for increasing the agricultural waste is their very high water content, yielding more metabolic activities in compare to the rest of other foods and cereals. The post-harvest metabolic activities continue and cause many fruits converting to fast-rotting products (Westerman et al., 1973). Therefore, drying can be used as one of the most important methods for large scale storing of fruits, because dried products can be stored for a long period without being rotted (Guine, 2006; Phuon et al., 2021). On the other hand, reducing the volume and weight of food after drying will facilitate their packaging, storage and transportation. The use of solar energy for drying foods and fruits has many disadvantages including inappropriate changes in the quality of the final product, lack of control over the drying process, long time of drying and insanitary final product (Yaldiz & Ertekin, 2001). Therefore, it is necessary to use modern and optimal methods in drying process of foods and agricultural crops (Defraeye & Radu, 2018).

Preharvest drop of pear fruits causes scratches and stains on the fruit and reduces its economic value. Therefore, instead of direct supply of the crop to the market, it can be processed and presented in a different and more valuable market. One of the most valuable methods for processing pears is drying (Guine, 2006). In this regard, numerous experimental and analytical studies have been carried out on the drying process of farm and garden crops. Doymaz (2004) studied drying and modeling carrot at four temperatures of 55, 60, 65, and 70°C and at an airflow rate of 1 and 1.5 m/s in laboratory drying. In this research, the best model for drying carrot was found (Doymaz, 2004).

Midilli and Kucuk (2003) performed kinetic modeling of drying thin-sliced of pistachios with and without skin using solar dryer with natural and forced airflow. The results of a comparative study of eight mathematical, semi experimental, and experimental models with experimental data showed that a logarithmic model and binomial model are applicable to describe the drying of pistachio with forced hot airflow and with natural airflow, respectively. Sharma et al. (2005) fitted 13 mathematical models using MATLAB software for modeling the drying kinetics of thin-sliced onions over the infrared drying process, and examined the models under investigation based on the explanatory factor (R^2), the root mean square error (RMSE) and sum of squared errors (SSE). According to their study, the model of Midilli et al. was selected as the best model for describing the drying kinetics of thin-sliced onions on the basis of statistical indices. Investigation of the drying kinetics of seeds of Hass avocado under different temperature conditions (313–353 K) showed that the Avhad and Marchetti model resulted better simulation of the drying kinetics of Hass avocado seeds in compare to the models of Lewis, Henderson, and Pabis and Page over the studied temperature range (Avhad & Marchetti, 2016). Defraeye and Radu (2018) examined the drying process of apple slices in a dryer by measuring the moisture content and shrinkage during drying. They concluded that by coupling the model of the hygrothermal history of the fruit during drying and the quality drop model, a better optimization of the drying process is obtained. Azeez et al. (2019) studied the kinetics of drying tomato slices (at temperatures of 30–120°C over 30 and 60 min) and found that the Page model ($R^2 = 0.9986$) was the best model for prediction of drying tomato slices. Proietti et al. (2018) have investigated the drying kinetics of pear by convective drying at 45–55°C. They reported that at 55°C, the faster drying rate and corresponding energy saving were obtained, with a more uniform water distribution in pear tissues. Their experimental data of moisture ratio during drying was well predicted by the diffusion model.

Understanding various steps of drying and the mass transfer mechanism at each stage is very important for better understanding the drying process of agricultural crops and foods. In this regard, by a comprehensive review of studies on the drying thin-sliced fruits, it has been distinguished that, despite numerous studies published in this field, there is no comprehensive and exact study on the different stages of the drying thin-sliced fruits. Exact determination of the boundaries of different drying areas, and study of the effect of different controllable parameters in each step to improve the drying velocity and the mass transfer coefficient are very important in designing and optimizing the new dryers with better performance. Moreover, in many studies on drying thin-sliced fruits, a diffusion coefficient is used for the entire drying process, which is far from the reality. Therefore, the purpose of this article is to investigate the different stages of drying of thin pears analytically and experimentally, as well as the effect of different stages of drying on the moisture ration, drying rate, effective moisture diffusivity, and shrinkage of pears.

2 | MATERIALS AND METHODS

2.1 | Drying test

In this research, a convective dryer was used to dry the thin-sliced pears. This dryer, with the exception of a variable-velocity centrifuge fan (1 hp/3000 rpm) for controlling the airflow rate, has four electric heaters with power of 2000 W and a number of temperature, humidity, and instantaneous sample weight measurement sensors. To achieve stable system conditions, all tests started 30 min after turning on the system. The specimens were then placed on the grid-shape tray of dryer (Khin et al., 2007). In order to perform the main experiment, the temperature of the dryer was changed at four levels in the range of 50, 60, 70, and 80°C and the air velocity of the intake air was 0.5, 1, and 1.5 m/s. To perform the tests, fresh Dargazi pear variety was obtained from fruit market. All specimens had skin and were kept in the refrigerator at a temperature of 4°C to reduce respiration and physiological and chemical changes. To study the kinetics of thin-sliced pears, samples were cut by a sausage slicer machine into thin-sliced with a diameter of 60 ± 5 mm and a thickness of 5 mm. The initial MC of the samples was determined by placing samples in an oven at 105°C until reaching a constant weight (Ertekin & Yaldiz, 2004; Guine, 2006).

2.2 | Modeling the drying kinetics of pear slices

At the beginning of the drying process, the pear slices are exposed to hot air and begin to heat up and after reaching a certain temperature, exchange mass with the fluid around them at a constant temperature, see Figure 1 (Adapted from Onwude et al., 2016). At this stage, the free and discontinuous water is evaporated from the outer surfaces of the pear slices and removed from the fruit without influence of the internal bulk materials and diffusivity properties. The energy required to evaporate surface water in this region is provided by hot air around the fruit slices and we have:

$$hA(T_\infty - T_w) = \dot{m}_w h_{fg} \tag{1}$$

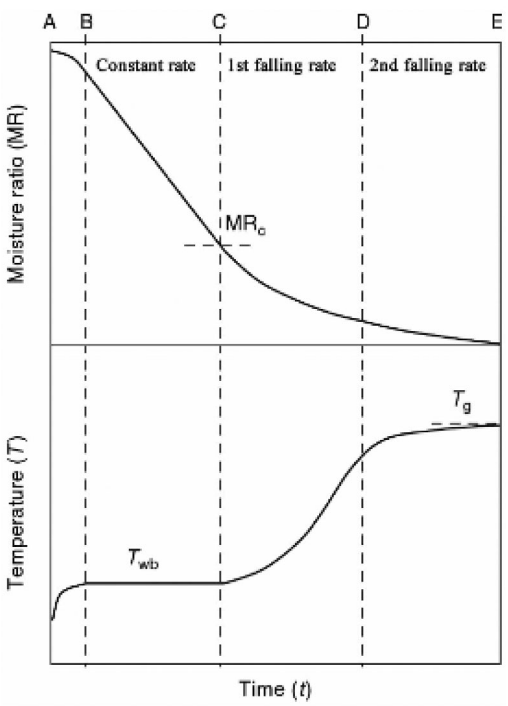

FIGURE 1 A representative drying temperature and moisture ratio (MR) of biomaterials (Adapted from Onwude et al. (2016))

where h is the convective heat transfer coefficient, A is the cross-sectional area of the exchange of heat and moisture of fruit with the surrounding air, T_∞ is the temperature of the hot air, T_w is the surface temperature of the sliced fruit, $\dot{m}_w$ is the mass of water evaporated from the free surface of the fruit per time, and h_{fg} is the latent heat of vaporization of water. On the other hand, the mass flux of water evaporated from the free surface of the sliced fruit ($\dot{m}_w$) depends on the free surface of the fruit (A) and the surface water vapor concentration (C_w) and the water vapor concentration of the airflow around the fruit (C_∞), which is related to these parameters by the mass transfer coefficient (K) (see Figure 2).

$$\dot{m}_w = KA(C_w - C_\infty) \tag{2}$$

Considering the rapid evacuation of water vapor from the free surfaces of the fruit in forced convection conditions (the fan is on), in practice, the concentration of water vapor in the airflow (C_∞) can be neglected and Equations (1) and (2) can be merged together, yielding

$$K = \frac{h(T_\infty - T_w)}{h_{fg} C_w} \tag{3}$$

Equation (3) shows that in the early stages of drying, the mass transfer coefficient (K) depends on the convective heat transfer coefficient (h), the hot air temperature (T_∞), and the initial MC (C_w). Therefore, theoretically, increasing the temperature and velocity of hot air at this stage of drying would significantly increase the mass transfer coefficient from free surfaces of the fruit.

In next step of drying the samples, the MC enclosed in the interior spaces of the fruit tissue and the internal cavities, that is, $M(x, t)$, reaches the surface of the sliced fruit and leaves it out, $C(x, t)$. This

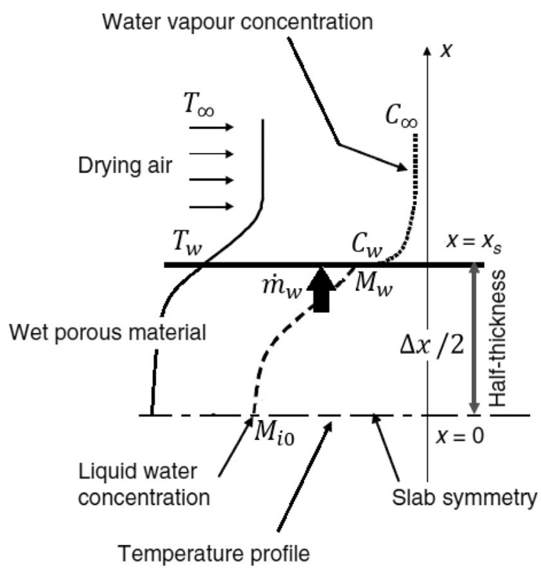

FIGURE 2 A schematic diagram illustrating the variation of internal moisture content (m_w), and water vapor concentration outside the dried materials (C_w).

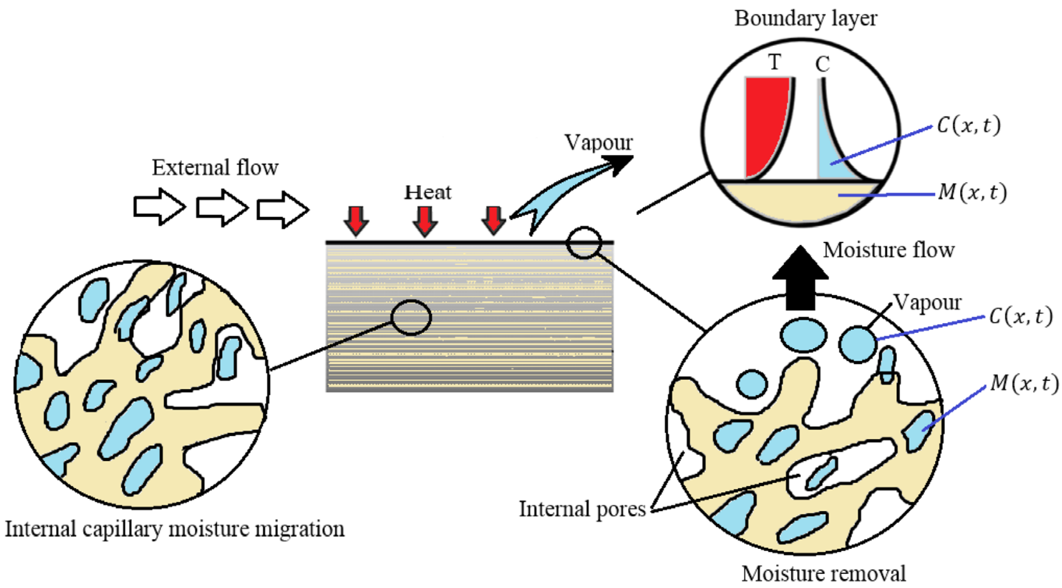

FIGURE 3 Schematic of the moisture content enclosed in the interior spaces of the fruit tissue, $M(x, t)$, and water vapor concentration at the surface of the sliced fruit $C(x, t)$

phenomenon is schematically illustrated in Figure 3. The moisture of this area is poorly bonded to the solid parts of the fruit tissue, therefore can be separated from the fruit tissue with consuming less energy. An example of a stereomicroscopic image of a drying sliced pear tissue is shown in Figure 1, illustrating the interstitial water enclosed in the interior of the pear tissue. At this stage of drying, the moisture transfer from the fruit tissue to its surface depends on the structure of the pores, the MC inside the fruit tissue and half of the thickness of the slices. These parameters are connected to each other by the following equation (see Figure 2).

$$\dot{m}_w = \frac{D_1 A}{\Delta x/2}(M_{i0} - M_w) \tag{4}$$

In Equation (4), D_1 is the moisture transfer coefficient in the second stage of drying, which is different with diffusion coefficient attributed for the third region of drying stage (D_{eff}), A is the moisture exchange surface of the sliced fruit, M_i is the MC of the fruit tissues (here M_{i0} is the moisture of center of slices), M_w is the MC of the fruit internal tissues close to the slab surface, and Δx is the thickness of the slices (see Figure 2). Relationship (4) shows that with increasing thickness of layers, the moisture transfer rate decreases. Moreover, according to Equation (4), by gradual decreasing the MC of the internal tissues of the fruit (M_i), the amount of moisture output flux from the internal tissues of the fruit decreases.

By continuing the drying process and semicontinuous evacuation of moisture from the internal tissue of the fruit, the continuation of moisture transfer from the internal tissues of the fruit to the outer surfaces and its evaporation is controlled through the diffusion phenomenon, which is inherently slow. In this region of drying, the transfer of moisture from the internal tissue of the fruit to the surface of the sliced fruit is difficult and needs more energy. In this region of the drying procedure, the Fick's second law is used to analyze the kinetics of drying thin-sliced fruit, which can be expressed as a differential equation with the second-order partial derivatives (Equation (5)) (Djebli et al., 2020).

$$\frac{\partial M}{\partial t} = D_{\text{eff}} \frac{\partial^2 M}{\partial x^2} \tag{5}$$

where M is the instant internal MC inside the fruit slice, t is the drying time, D_{eff} is the moisture diffusion coefficient (m^2/s), M_e is the equilibrium MC, and M_o is the average initial MC at the fruit internal tissues.

The Fick's second law (Equation (5)) is true for conditions where moisture from the internal parts of the fruit to the outside is driven by the diffusion phenomenon and changes in the physical properties of the drying slices, such as internal porosity or tissue stiffness, are negligible. Moreover, the moisture released from the surface of the product is continuously removed from the outer surface of the drying slices. In other words, the moisture transferred to the outer surfaces of the fruit does not accumulate in the form of water vapor at the surface of the sliced fruit. According to the existing conditions, this relationship can be used for the descending step of the drying process of the sliced pears. The solution of Equation (5) is presented by Crank as the following equation (Equation (6)) (Zadhossein et al., 2022).

$$MR(x,t) = \frac{M - M_e}{M_{D0} - M_e} = \frac{8}{\pi^2} \sum_{n=0}^{\infty} \frac{1}{(2n+1)^2} \exp\left(-\frac{(2n+1)^2 \pi^2 D_{\text{eff}}\, t}{4L^2}\right) \sin\left(\frac{(2n+1)\pi x}{L}\right) \tag{6}$$

In this equation, MR is the moisture ratio (dimensionless), and L is the thickness of the sliced pears to be dried ($\Delta x = L$). For dimensionless drying time; $= \left({}^{\alpha t}/_{L^2}\right) > 0.2$, ($\alpha$ stands for diffusion coefficient of the

TABLE 1 Models used for fitting experimental data of MR

	Model name	Model	Reference
1	Newton	$MR = \exp(-kt)$	İlter et al. (2018)
2	Page	$MR = \exp(-kt^n)$	Li, Chen, et al. (2021) and Li, Li, et al. (2021)
3	Henderson and Pabis	$MR = a.\exp(-kt)$	Çetin (2022)
4	Logarithmic	$MR = a.\exp(-kt) + c$	Manzoor et al. (2021)
5	Two-term	$MR = a.\exp(-k_0 t) + b.\exp(-k_1 t)$	Jafari et al. (2017)
6	Wang and Singh	$MR = 1 + at + bt^2$	Rashid et al. (2020)
7	Approximation of diffusion	$MR = a.\exp(-kt) + (1-a)(-kbt)$	Okonkwo et al. (2021)
8	Midilli et al.	$MR = a.\exp(-kt^n) + bt$	El-Mesery et al. (2023)

Abbreviation: MR, moisture ratio.

samples), the first sentence of the above series, by placing $n = 0$ in Equation (6), can be used to calculate the MC of the pears during the drying process. Based on research conducted on biomaterials such as pears with high MC, the measurement of the equilibrium MC (M_e) is not necessary in computing the moisture ratio (MR), (Doymaz, 2007), so after integrating over the thickness of drying samples we will have.

$$MR \cong \frac{M_t}{M_0} = \frac{8}{\pi^2} \exp\left(-\frac{\pi^2}{4L^2} D_{\text{eff}}\, t\right) \tag{7}$$

Similar to Equation (7), several modified models have been proposed and developed by researchers (see Table 1). For example, the model presented by Henderson and Pabis is structurally close to Equation (7). Therefore, in the present study, instead of plotting Equation (7), the improved and modified equations presented in Table 1 have been used to check the MC of the sliced pears. For each drying temperature, the equations of Table 1 were extracted and the mean accuracy index of the fitting at different temperatures was obtained for each model. Then, the obtained equations were compared with each other and the superior model was chosen. For superior models, coefficients and constants were obtained at different temperatures, and finally the graph of the drying curve related to the pear slices was plotted.

In this study, three factors of R^2, RMSE, and SSE were used to determine the best model presented in Table 1 to predict changes in the moisture fraction of the sliced pears versus time (Li, Chen, et al., 2021; Li, Li, et al., 2021). In the following, experimental models were used to fit data obtained from drying under the mentioned conditions. The best fit that can characterize the drying of thin-sliced pears is a model with the maximum correlation coefficient of R^2 and the lowest RMSE and SSE (Li, Chen, et al., 2021; Li, Li, et al., 2021). For this purpose, Equations (8)–(10) were used, and a summary of the calculations is presented in Section 3 (Table 2). MATLAB software version R2013a was used to evaluate the fitting of standard drying models.

$$R^2 = \frac{\sum_{i=1}^{n}(MR_i - MR_{\text{pre},i}) \cdot \sum_{i=1}^{n}(MR_i - MR_{\exp,i})}{\sqrt{\left[\sum_{i=1}^{n}(MR_i - MR_{\text{pre},i})^2\right]\left[\sum_{i=1}^{n}(MR_i - MR_{\exp,i})^2\right]}} \tag{8}$$

TABLE 2 Average values of R^2, RMSE, and SSE for the studied models in the present study

Models	R^2	RMSE	SSE
Newton	0.9891	0.0221	0.1208
Page	0.9961	0.0146	0.0543
Henderson and Pabis	0.9924	0.0205	0.1075
Logarithmique	0.9971	0.0125	0.0446
Two-term	0.9929	0.0199	0.0942
Wang and Singh	0.9958	0.0162	0.0530
Approximation of diffusion	0.9926	0.0162	0.1000
Midilli et al.	0.9989	0.0080	0.0157

Abbreviation: RMSE, root mean square error.

$$\text{RSME} = \left(\frac{1}{N}\sum_{i=1}^{n}(MR_{\text{pre},i} - MR_{\exp,i})^2\right)^{\frac{1}{2}} \tag{9}$$

$$\text{SSE} = \frac{1}{N}\sum_{i=1}^{n}(MR_{\exp,i} - MR_{\text{pre},i})^2 \tag{10}$$

So that $MR_{\exp,i}$ is the experimental moisture fraction, $MR_{\text{pre},i}$ is the ith predicted moisture fraction, and N is the number of observations.

2.3 | Effective moisture diffusion coefficient inside the sliced pears during drying and their activation energy

In order to obtain the effective moisture diffusion coefficient inside the sliced pears, the logarithms of both sides of Equation (7) can be taken (Kaveh et al., 2022):

$$\ln(MR) = \ln\left(\frac{8}{\pi^2}\right) - \left(\frac{\pi^2}{4L^2} D_{\text{eff}}\, t\right) \tag{11}$$

By drawing the natural logarithm of moisture ratio (ln(*MR*)) vs. the time (*t*), a line with the slop of k_1 is obtained that the D_{eff} can easily be obtained.

$$k_1 = \frac{\pi^2}{4L^2} D_{\text{eff}} \tag{12}$$

The coefficient of k_1 (rate or coefficient of drying) is more noticeable due to its more simple dimension in compare to the effective diffusion coefficient (D_{eff}).

In the following, in order to study the effect of drying temperature on the variation of the effective moisture diffusion coefficient, Arrhenius's equation (Equation (13)) is used (Hadibi et al., 2021).

$$D_{\text{eff}} = D_0 \exp\left(\frac{-E_a}{R} \cdot \frac{1}{T}\right) \tag{13}$$

In Equation (13), D_0 is the constant coefficient of exponential function, E_a is the activation energy, and R is the global constant of the gas constant. In order to obtain the activation energy of the sliced pears during drying and the variations in the effective moisture diffusion coefficient versus the drying temperature, the logarithms of both sides of Equation (13) can be taken:

$$\ln(D_{\text{eff}}) = \ln(D_0) - \left(\frac{E_a}{R}\right)\frac{1}{T} \tag{14}$$

Plotting the natural logarithm of the D_{eff} (ln(D_{eff})) versus the inverse of the drying temperature (1/*T*), results a line with a constant slop ($\frac{E_a}{R}$), which can easily be used to obtain the activation energy.

2.4 | Study of shrinkage kinetics

To evaluate the shrinkage of the samples during drying, a digital camera (Webcam-7-Pro_1.0.5.2) was placed above the suspended lace containing the drying samples to provide imaging at the velocity of one frame per minute from samples and saving photos in the computer without removing the samples from the dryer (Guarte, 1996). Image J software was used to extract shrinkage-related information such as image surface. The percentage of shrinkage at each time of drying was calculated by the following equation (Nwakuba et al., 2021):

$$\frac{d(sh)}{dt}\% = \left(1 - \frac{d(A_t)/dt}{A_0}\right) \times 100 \tag{15}$$

where *sh* is the shrinkage, A_0 is surface area of the sample before drying, and A_t is the instant sample area during drying at the time of *t*.

3 | RESULTS AND DISCUSSION

To evaluate kinetics models related to the drying of thin-sliced pears, data resulted from drying were converted to moisture ratio (MR) data, and these data along with drying time data in minutes were fitted using the eight models presented in Table 1. To select the best model, values of R^2, RMSE, and SSE were calculated using the Equations (8)–(10) based on the observed data. The range of variations of values of R^2, RMSE, and SSE is presented in Table 2.

The results obtained in this study (Table 2) showed that experimental data related to the kinetics of drying pears layers were satisfactorily fitted by the Midilli et al. model. In this regard, Karimi et al. (2021) proposed the Midilli et al. model as the best model for drying of Gundelia tournefortii L. sheets among 10 models. Moreover, Mirzaee Ghale et al. (2009) introduced the regression model of Midilli et al. as the best model for predicting moisture fraction of apricot fruit layers.

In the following, Figure 4 shows the changes in the MR resulting from the drying of thin-sliced pears variety of Dargazi with 5 mm thickness in four temperature levels of 50–80°C and three levels of air velocity of 0.5–1.5 m/s along with the results of the prediction of the Midilli et al. model. According to the results shown in Figure 4, experimental data and data obtained using the Midilli model are very similar, so that the curve related to the experimental and curve related to data derived from the Midilli model are overlapped each other. Regarding the evaluation indicators of the regression model presented in Table 2, it is clear that the Midilli et al. model provides better prediction for the drying thin-sliced pears. According to the results shown in Figure 4, it can be said that at the higher air temperature of dryer, the MC decreases faster in the first minutes of the drying, which is consistent with the findings of other researchers (Li, Chen, et al., 2021; Li, Li, et al., 2021; Okonkwo et al., 2021; Zhao et al., 2021). Therefore, the highest drying velocity is at 80°C and at an airflow velocity of 1.5 m/s. Similar results have been reported by Doymaz (2004) on carrots, okra, and tomatoes (Doymaz, 2007).

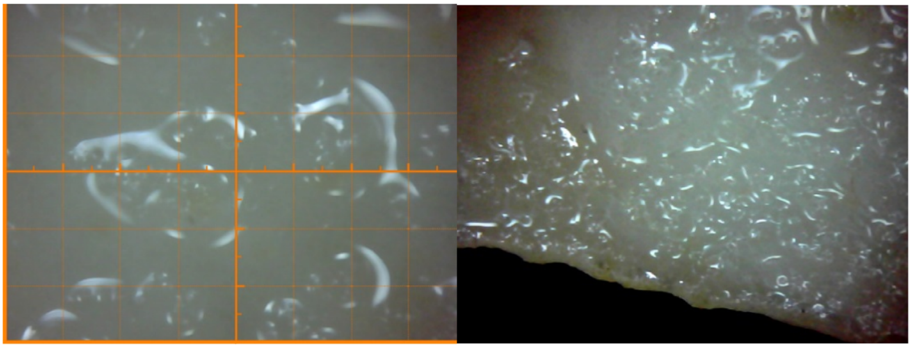

FIGURE 4 The stereomicroscopic image of the outer surface of the sliced tissue of pear fruit at the beginning of drying with large and interconnected layers of water (right), the stereomicroscopic image of the sliced pear fruit section after entering the second region of drying with smaller interstitial water layers (left)

Another noteworthy point is that the most parts of MR curve at low airflow velocity (0.5 and 1 m/s) and high temperatures of 70 and 80°C are overlapped each other, while at high airflow velocity (1.5 m/s), the slope of the variation of these two curves is completely different. The reason for this can be insufficient drainage of moisture reaching the surface of the fruit at low airflow rate and high drying temperatures. Simply, at higher drying temperatures, the amount of moisture transferred to the surface of the sliced fruit increases. However, if the airflow velocity is not sufficient around the fruit, this MC cannot drained from the outer surfaces of the fruit and remains on the surface of the sliced fruit, causing reduction of the mass transfer rate. As airflow rate increases, the rate of moisture evacuation from the outer surfaces of the slices increases and as a result, the moisture fraction curve corresponding to the temperature of 80°C is placed below the moisture fraction curve of temperatures up to 70°C.

3.1 | Variation of drying rate versus MC

Curves related to changes in drying rate versus reducing the MC of the pear slices for different drying temperatures are shown in Figure 5. According to the results shown in Figure 5, the drying rate of thin pear samples can be divided into three distinct regions. In the first region, which is from the start of the drying process (initial MC of 87%) to 57% MC, curve concavity is positive and upward representing a higher drying rate. At this stage, the free and discontinuous water evaporates from the free surfaces of the cut layer and is removed from the fruit.

In the second region of drying (from 57 to 27% MC), the slope of the drying rate variations is lower than the other two regions, especially at lower airflow rate. With increasing airflow rate and drying temperature, the slope of the drying rate also increases in this area (Figure 5). In the second region of drying, the water entrapped in the interior of the fruit tissues and the internal cavities reaches the surface of the sliced fruit. The water of this region is poorly bonded to the solid tissue of the fruit and can be separated from it by less energy. The stereomicroscopic image of a drying sliced pear tissue, shown in Figure 6, illustrates the interstitial water enclosed in the interior part of the pear fruit tissue. According to the results shown in Figure 5, in the second region of drying, the drying curves at 70 and 80°C are very close to each other in the flow rate of 0.5 and 1 m/s.

In the third region (from MC of 27% to the final drying moisture), curvature of the drying rate is negative and downward indicating that the rate of drying is reducing (Figure 5). In this area of drying, the transfer of moisture from the internal tissue to the surface of the fruit slices is controlled by diffusion phenomenon, which is very slow and requires more energy. The negative concavity related to the curve of the variation of the drying rate also reflects the same concept. According to the results shown in Figure 5, MC of 27% is considered as the critical MC of the sliced pears, so that the downward curvature variations of the drying curve can be observed in this moisture.

3.2 | Variation of diffusion coefficient in different areas of drying of thin-sliced pears

The average natural logarithmic variation of the D_{eff} versus the inverse of the drying temperature for the third drying region has been shown in Figure 8. In most studies in the field of drying thin-sliced fruits, a D_{eff} is used for the entire drying process, which is far from the reality. Such a hypothesis provides a relatively acceptable approximation for drying biomaterials such as rough rice or corn seeds that during drying, a large part of their moisture reaches to the outer surface of the grain through diffusion, but it is not a suitable factor in drying biomaterials such as thin sliced fruits with high surface moisture in slice sections. By comparing the linear equations fitted with Equation (14), intercept of the fitted equations is equal to $\ln(D_0)$ and the slope of the line represents $\frac{E_a}{R}$. According to the results shown in Figure 7, the numerical value of $\ln(D_{eff})$ decreases with the inverse increase in the drying temperature. In other words, by increasing the drying temperature, the natural logarithm of the D_{eff} is increasing and as a result, the D_{eff} increased. Typically, with an increase in the drying temperature from 50 to 60°C at an air velocity of 0.5 m/s, the effective diffusion coefficient increases from 1.19×10^{-7} to 4.09×10^{-7}. Similar results were obtained by other researchers (see, e.g., Deng et al., 2020; İlter et al., 2018; Okonkwo et al., 2021). Another noticeable point of the results shown in Figure 7 is that the logarithmic curve of the effective diffusion coefficient corresponding to the air velocity of 1.5 m/s is below the rest of the graphs and shows that the increase of the flow rate of the input air in the third stage of drying not only increases the mass transfer rate from the sliced pears, but also reduces the effective mass transfer coefficient. This is very important in reducing the energy consumed in drying the thin-sliced pears and possibly other fruits, because the increase in the airflow rate in the third stage of the drying curve not only does not increase the drying rate, but also increases the drying costs. This result is very important for energy management for reducing the cost of producing fruit chips. According to the results presented in Figure 7, the maximum D_{eff} in the third region of drying the thin-sliced pears is 6.25×10^{-7}, which was obtained at the drying temperature of 80°C and the flow rate of 0.5 m/s. Moreover, the lowest D_{eff} was equal to 7.71×10^{-8}, which was related to the drying temperature of 50°C and the air velocity of 1.5 m/s.

3.3 | Investigating the shrinkage rate of pear slice samples during drying

The variations in the shrinkage rate of the thin-sliced pears versus the MC of the sample have been presented in Figure 8. A very interesting point in these diagrams is that the shrinkage rate also has three distinct regions, similar to the drying rate-MC graphs:

1. First region of shrinkage from initial MC up to moisture of 57%.
2. Second region of shrinkage from MC of 57% to moisture of 27%.

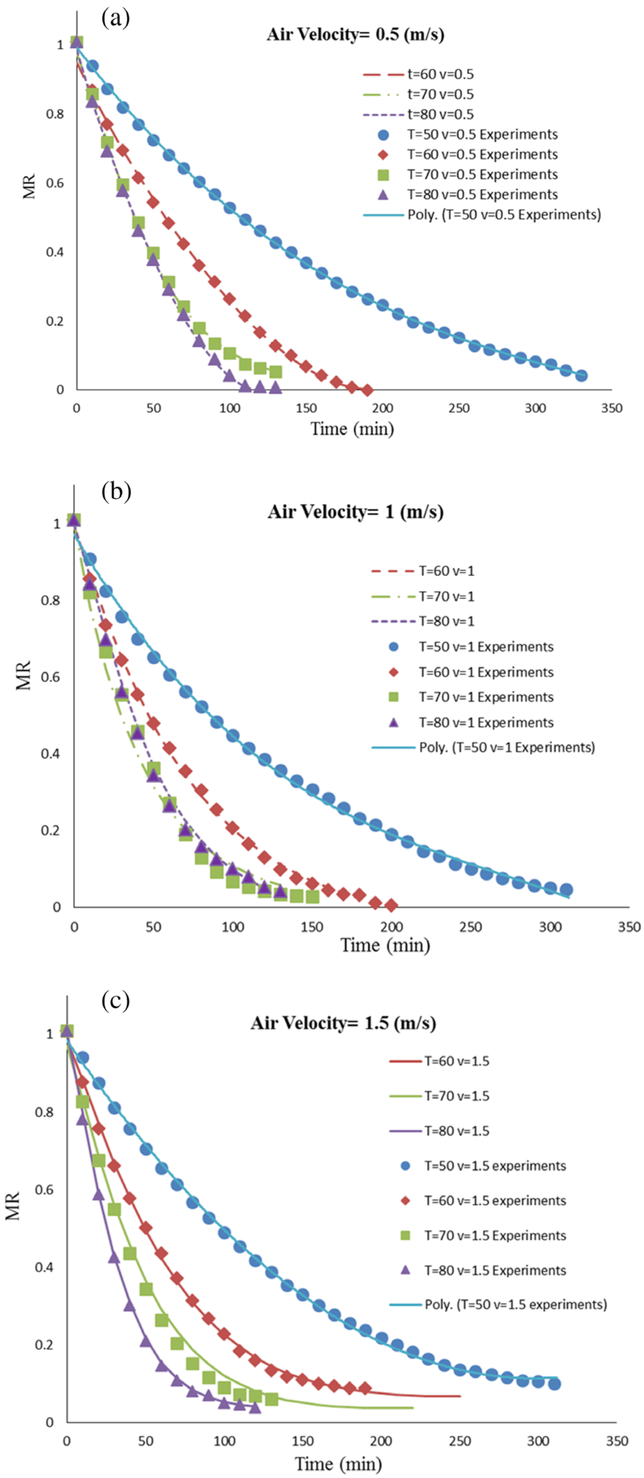

FIGURE 5 Changing the moisture fraction during drying at different temperatures resulted by experimental data and the Midilli et al. model at air velocity of (a) 0.5 m/s, (b) 1 m/s, and (c) 1.5 m/s (c)

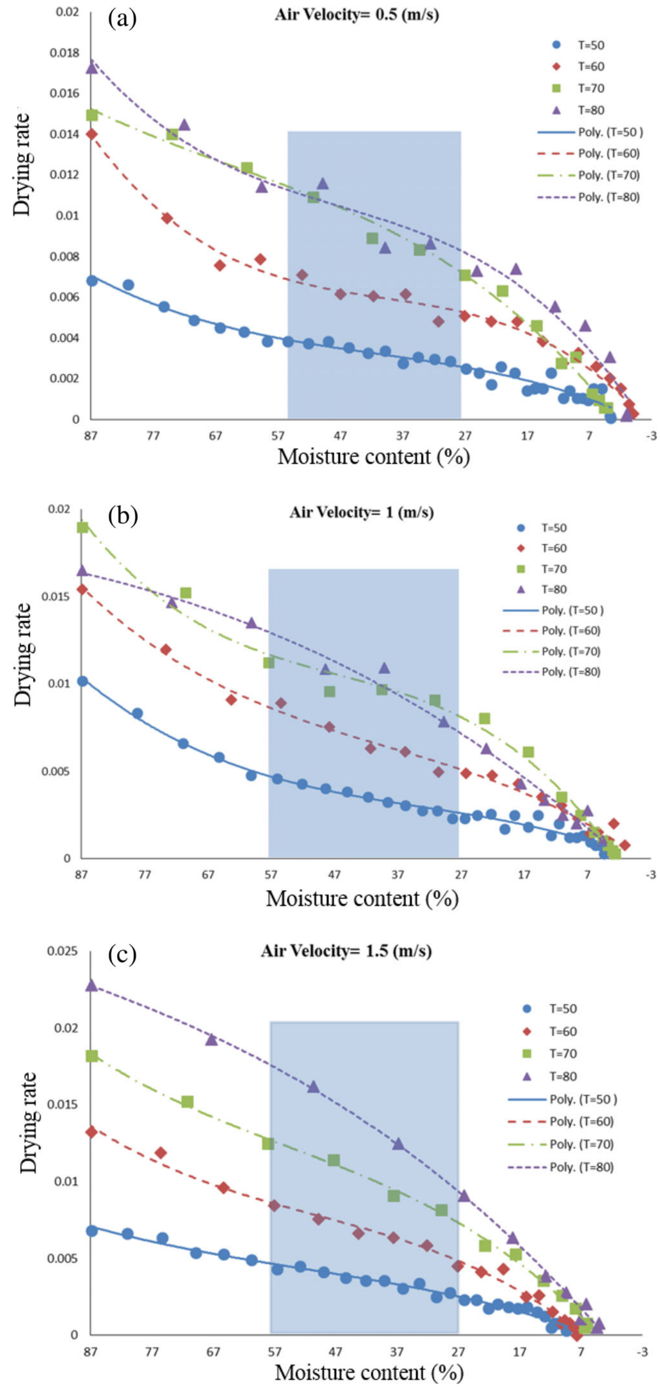

FIGURE 6 Changes in the drying rate versus moisture content during drying with different temperatures from experimental data at air velocity of (a) 0.5 m/s, (b) 1 m/s, and (c) 1.5 m/s (c)

3. Third region of shrinkage from MC of 27% to final moisture (full drying of fruit).

In the first region, the shrinkage rate of the sliced pears (except the drying temperature of 80°C at an airflow velocity of 0.5 m/s) has the positive slope, whereas in the third region, the slop is negative. In the second region of the shrinkage, the slope of the variation is less than the other two regions, and in most cases its slope is negligible and nonsignificant, indicating constant shrinkage variation versus the MC of the samples. In the first region of the shrinkage rate, which is from the beginning of drying process (initial MC of 87%) to 57% MC, curvature of the curve is upward and positive. In the second region of the shrinkage rate (from 57% moisture to 27% moisture), the variation

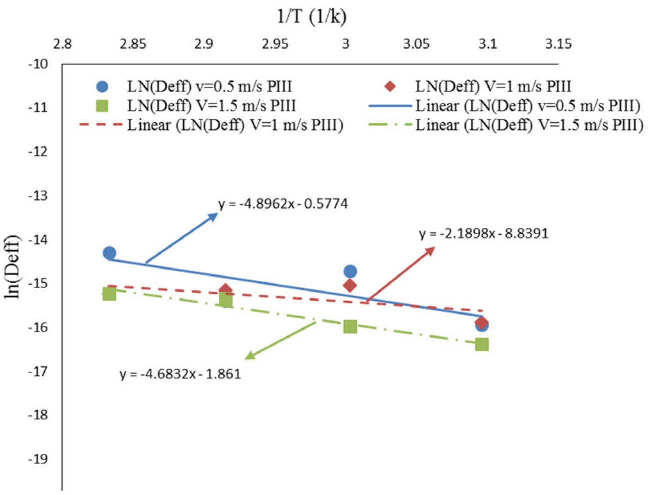

FIGURE 7 Variation of average natural logarithm of effective diffusion coefficient versus the inverse of drying temperature

of the curve in most cases is constant. In the third region of the drying rate-shrinkage rate curve (from 27% moisture to the final step of drying MC), the curvature of the curve is negative and downward, which indicates a decrease in the rate of shrinkage. In this area of drying, the transfer of moisture from the internal tissue of the fruit to the surface of the fruit slices is very slow and consequently less shrinkage rate was observed.

In the following, the variation of surface shrinkage of pear sheets during drying as a function of drying temperature are shown in Figure 9. In this figure, the shrinkage of the pear slices has been presented for temperatures of 50, 60, 70, and 80°C, air velocity of 0.5, 1, and 1.5 m/s and a specimen thickness of 5 mm. According to the results shown in Figure 9, the percentage of shrinkage of pear layers increases with increasing drying temperature and consequently decreasing MC. The reason for this phenomenon is the reduction of viscoelasticity stresses in the pores due to the loss of moisture, consequently the reduction of pressure in the internal pores and vertebral pores (Goplour et al., 2017; Sufer et al., 2019; Joudi- Sarighayeh et al., 2022). According to the results shown in Figure 9, temperature variations have a greater influence on the process of loss of moisture and shrinkage, compared to the flow rate of the inlet air.

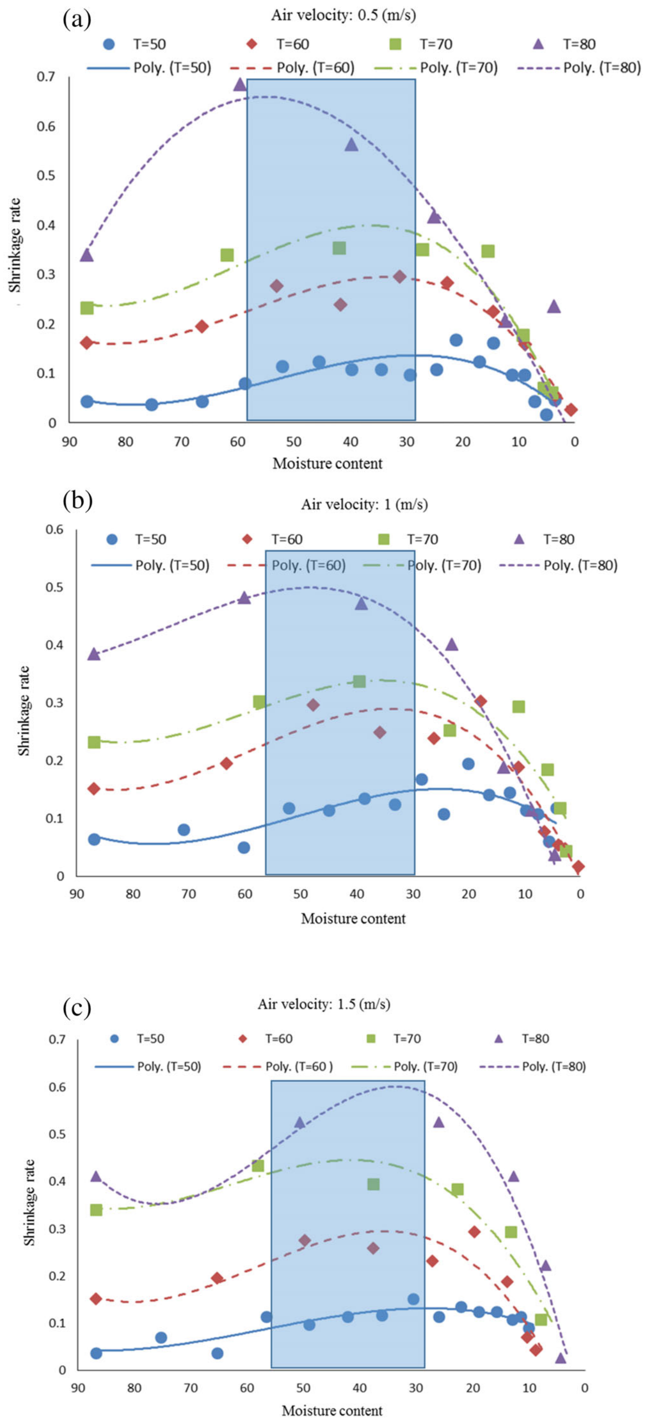

FIGURE 8 Variation of shrinkage rate versus moisture content during drying with different temperatures obtained from experimental data: (a) air velocity of 0.5 m/s, (b) air velocity of 1 m/s, and (c) airflow velocity 1.5 m/s

4 | CONCLUSION

In this research, the influence of different parameters of a convective hot air dryer on the mass transfer coefficients was investigated in different drying regions of thin-sliced pears, including drying temperature and air velocity of the input air, along with the physical characteristics of the drying product. The results of experimental data analysis showed that the model proposed by Midilli et al., has the best fitting statistical indexes among the eight different examined models for drying process of thin-sliced pear fruit. For the model proposed by Midilli et al., the statistical indices of R^2, RMSE, and SSE were 0.9989, 0.008, and 0.0157, respectively. According to the results of this study, drying temperature and airflow rate had the most and least effect on the shrinkage of thin-sliced pears, respectively. The results of this study showed that if the drying temperature increases to 80°C, it is necessary to increase the air velocity to 1.5 m/s until reaching the critical MC of the pear (27% for drying the examined pear slices). Otherwise, at a flow velocity of 1 m/s or less, the difference between the drying curves at 70 and 80°C would not be significant, with the

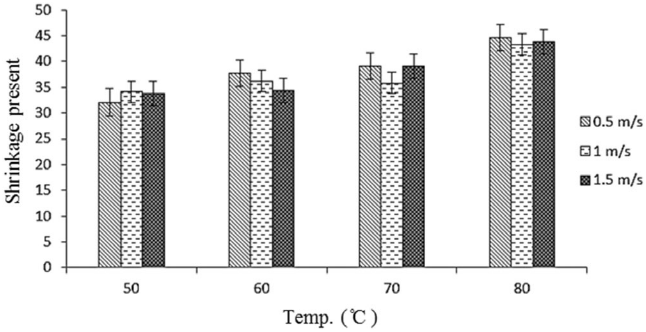

FIGURE 9 Changes in the surface shrinkage of pear sheets during drying as a function of drying temperature and air velocity

exception that at a drying temperature of 70°C, less energy is consumed and economically is justifiable. After reducing the MC of the pear slices to the critical moisture, that is, 27%, the drying temperature of 80°C and the flow velocity of 0.5 m/s is recommended. Increasing the flow rate of the input air in the third stage of drying, not only does not increase the mass transfer rate of the sliced pears, but also reduces the effective mass transfer coefficient. This founding is completely different with the predictions of just simply using the popular average dimensionless mass transfer coefficient represented by Sherwood number in the form of $Sh = C_1 Re^a Sc^b$, which is true for estimating the mass transfer coefficient for the whole drying range and may not valid for describing only the third region of drying biomaterials. Since the mass transfer phenomenon in the third region of drying is not very sensitive to the *Re* number of flowing fluids around the samples. In this relationship, *Sh* stands for the Sherwood number ($Sh = h_m L / D_{eff}$) and *Sc* is the Schmitt number defined by $Sc = \upsilon / D_{eff}$. It seems that applying treatments such as low-power microwaves or infrared wavelengths in the third stage of drying can assist increasing the moisture diffusion coefficient in this region, which is the subject of future study and would be of interest to other researchers.

CONFLICT OF INTEREST

The authors declare no potential conflict of interest.

DATA AVAILABILITY STATEMENT

The data that support the findings of this study are available from the corresponding author upon reasonable request.

ORCID

Davood Kalantari https://orcid.org/0000-0002-4118-2918
Mohammad Kaveh https://orcid.org/0000-0001-5285-2211
Mohsen Azadbakht https://orcid.org/0000-0002-5726-9321
Esmail Khalife https://orcid.org/0000-0002-1690-1714

REFERENCES

Avhad, M. R., & Marchetti, J. M. (2016). Mathematical modelling of the drying kinetics of Hass avocado seeds. *Industrial Crops and Products*, *91*, 76–87.

Azeez, L., Adebisi, S. A., Oyedeji, A. O., Adetoro, R. O., & Tijani, K. O. (2019). Bioactive compounds' contents, drying kinetics and mathematical modelling of tomato slices influenced by drying temperatures and time. *Journal of the Saudi Society of Agricultural Sciences*, *18*(2), 120–126.

Çetin, N. (2022). Prediction of moisture ratio and drying rate of orange slices using machine learning approaches. *Journal of Food Processing and Preservation*, *46*(11), e17011.

Defraeye, T., & Radu, A. (2018). Insights in convective drying of fruit by coupled modeling of fruit drying, deformation, quality evolution and convective exchange with the airflow. *Applied Thermal Engineering*, *129*, 1026–1038.

Deng, L.-Z., Mujumdar, A. S., Yang, W.-X., Zhang, Q., Zheng, Z.-A., Wu, M., & Xiao, H.-W. (2020). Hot air impingement drying kinetics and quality attributes of orange peel. *Journal of Food Processing and Preservation*, *44*(1), e14294.

Djebli, A., Hanini, S., Badaoui, O., Haddad, B., & Benhamou, A. (2020). Modeling and comparative analysis of solar drying behavior of potatoes. *Renewable Energy*, *145*, 1494–1506.

Doymaz, I. (2004). Convective air drying characteristics of thin layer carrots. *Journal of Food Engineering*, *61*, 359–364.

Doymaz, I. (2007). Air-drying characteristics of tomatoes. *Food. Engineering*, *78*, 1291–1297.

EL-Mesery, H. S., Tolba, N. M., & Kamel R. M. (2023). Mathematical modelling and performance analysis of airflow distribution systems inside convection hot-air dryers. *Alexandria Engineering Journal*, *62*, 237–256.

Ertekin, C., & Yaldiz, O. (2004). Drying of eggplant and selection of a suitable thin layer drying model. *Journal of Food Engineering*, *63*, 349–360.

Goplour, I., Nejad, M. Z., Chayjan, R. A., Nikbakht, A. M., Guine, R. P. F., & Dowlati, M. (2017). Investigating shrinkage and moisture diffusivity of melon seed in a microwave assisted thin layer fluidized bed dryer. *Journal of Food Measurement and Characterization*, *11*, 1–11.

Guarte, R. C. (1996). *Modelling the drying behavior of copra and development of a natural convection dryer for production of high quality copra in The Philippines* (Ph.D. Dissertation). Hohenheim University.

Guine, R. (2006). Influence of drying method on density and porosity of pears. *Food and Bioproducts Processing*, *84*, 179–185.

Hadibi, T., Boubekri, A., Mennouche, D., Benhamza, A., Besombes, C., & Allaf, K. (2021). Solar–geothermal drying/instant controlled pressure drop-swell drying of mechanically dewatered tomato paste. *Journal of Food Process Engineering*, *44*(10), e13811. https://doi.org/10.1111/jfpe.13811

İlter, I., Akyıl, S., Devseren, E., Okut, D., Koç, M., & Ertekin, F. K. (2018). Microwave and hot air drying of garlic puree: Drying kinetics and quality characteristics. *Heat and Mass Transfer*, *54*, 2101–2112.

Jafari, H., Kalantari, D., & Azadbakht, M. (2017). Semi-industrial continuous band microwave dryer for energy and exergy analyses, mathematical modeling of paddy drying and it's qualitative study. *Energy*, *138*, 1016–1029.

Joudi-Sarighayeh, F., Abbaspour-Gilandeh, Y., Kaveh, M., & Hernández-Hernández, J. L. (2022). The optimization of the physical–thermal and bioactive properties of pumpkin slices dried in a hybrid microwave–convective dryer using the response surface method. *Agronomy*, *12*(10), 2291. https://doi.org/10.3390/agronomy12102291

Karimi, S., Layeghinia, N., & Abbasi, H. (2021). Microwave pretreatment followed by associated microwave-hot air drying of Gundelia tournefortii L.: Drying kinetics, energy consumption and quality characteristics. *Heat and Mass Transfer*, *57*, 133–146.

Kaveh, M., Taghinezhad, E., Witrowa-Rajchert, D., Imanian, K., Khalife, E., & Nowacka, M. (2022). Use of ultrasound pre-treatment before microwave dryingof kiwifruits – An optimization approach with response surface methodology. *Journalof Food Processing Preservation*, *46*(7), e16714.

Khin, M., Zhou, W., & Yeo, S. Y. (2007). Mass transfer in the osmotic dehydration of coated apple cubes by using maltodextrin as the coating material and their textural properties. *Journal of Food Engineering*, *8*(1), 514–522.

Li, M., Chen, Y., Geng, Y., Liu, F., Guo, L., & Wang, X. (2021). Convenient use of low field nuclear magnetic resonance to determine the drying

kinetics and predict the quality properties of mulberries dried in hot-blast air. *LWT*, *137*, 110402.
Li, X., Li, J., Wang, R., Rahaman, A., Zeng, X.-A., & Brennan, C. S. (2021). Combined effects of pulsed electric field and ultrasound pretreatments on mass transfer and quality of mushrooms. *LWT*, *150*, 112008.
Manzoor, A., Khan, M. A., Mujeebu, M. A., & Shiekh, R. A. (2021). Comparative study of microwave assisted and conventional osmotic dehydration of apple cubes at a constant temperature. *Journal of Agriculture and Food Research*, *5*, 100176.
Midilli, A., & Kucuk, H. (2003). Mathematical modeling of thin layer drying of pistachio by using solar energy. *Energy Conversion and Management*, *44*, 1111–1122.
Mirzaee Ghale, M., Rafiee, S., Keihani, A., Emam Jomeh, Z., & Taheri Geravand, A. (2009). Modeling thin layer drying of apricot. *Electronic Journal of Food Processing and Maintenance*, *1*(2), 139–150.
Nwakuba, N., Ndukwe, S., & Paul, T. (2021). Influence of product geometry and process variables on drying energy demand of vegetables: An experimental study. *Journal of Food Process Engineering*, *44*(6), e13684. https://doi.org/10.1111/jfpe.13684
Okonkwo, C. E., Olaniran, A. F., Adeyi, O., Adeyi, A. J., Ojediran, J. O., Adewumi, A. D., Iranloye, Y. M., & Erinle, O. C. (2021). Drying characteristics of fermented-cooked cassava chips used in the production of complementary food: Mathematical and Gaussian process regression modeling approaches. *Journal of Food Process Engineering*, *44*(7), e13715. https://doi.org/10.1111/jfpe.13715
Onwude, D. I., Hashim, N., Janius, R. B., Nawi, N. M., & Abdan, K. (2016). Modeling the thin-layer drying of fruits and vegetables: A review. *Comprehensive Reviews in Food Science and Food Safety*, *15*, 599–618.
Phuon, V., Ramos, I. N., Brandao, T. R. S., & Silva, C. L. M. (2021). Assessment of the impact of drying processes on orange peel quality characteristics. *Journal of Food Process Engineering*, *45*(7), e13794. https://doi.org/10.1111/jfpe.13794
Proietti, N., Adiletta, G., Russo, P., Buonocore, R., Mannina, L., Crescitelli, A., & Capitani, D. (2018). Evolution of physicochemical properties of pear during drying by conventional techniques, portable-NMR, and modelling. *Journal of Food Engineering*, *230*, 82–98.
Qu, H., Islam, M. M. M. M., Khan, M. I. H., Ananno, A. A., & Karim, A. (2021). Sustainable food drying technologies based on renewable energy sources. *Critical Reviews in Food Science and Nutrition*, *62*, 6872–6886. https://doi.org/10.1080/10408398.2021.1907529
Rashid, M. T., Jatoi, M. A., Safdar, B., Wali, A., Aadil, R. M., Sarpong, F., & Ma, H. (2020). Modeling the drying of ultrasound and glucose pretreated sweet potatoes: The impact on phytochemical and functional groups. *Ultrasonics Sonochemistry*, *68*, 105226.
Sharma, G. P., Verma, R. C., & Pathare, P. B. (2005). Thin-layer infrared radiation drying of onion slices. *Journal of Food Engineering*, *67*, 361–366.
Sufer, O., & Palazoglu, T. K. (2019). A study on hot-air drying of pomegranate kinetics of dehydration, rehydration and effects on bioactive compounds. *Journal of Thermal Analysis and Calorimetry*, *137*, 1981–1990.
Westerman, P. W., White, G. M., & Ross, I. J. (1973). Relative humidity effect on the high temperature drying of shelled corn. *Transactions of the ASAE*, *16*, 1136–1139.
Yaldiz, O., & Ertekin, C. (2001). Thin layer solar drying of some vegetables. *Drying Technology*, *19*, 583–596.
Zadhossein, S., Abbaspour-Gilandeh, Y., Kaveh, M., Kalantari, D., & Khalife, E. (2022). Comparison of two artificial intelligence methods (ANNs and ANFIS) for estimating the energy and exergy of drying cantaloupe in a hybrid infrared-convective dryer. *Journal of Food Processing and Preservation*, *46*(10). Portico. https://doi.org/10.1111/jfpp.16836
Zhao, C.-C., Ameer, K., & Eun, J.-B. (2021). Effects of various drying conditions and methods on drying kinetics and retention of bioactive compounds in sliced persimmon. *LWT*, *143*, 111149.

How to cite this article: Kalantari, D., Naji-Tabasi, S., Kaveh, M., Azadbakht, M., Majnooni, M., Khorshidi, Y., Asghari, A., & Khalife, E. (2022). Drying kinetics and shrinkage rate of thin-sliced pears in different drying stages. *Journal of Food Process Engineering*, e14264. https://doi.org/10.1111/jfpe.14264